Dye-Sensitized Solar Cells

DOI: 10.1002/anie.201006635

Low-Cost Molybdenum Carbide and Tungsten Carbide Counter Electrodes for Dye-Sensitized Solar Cells**

*Mingxing Wu, Xiao Lin, Anders Hagfeldt, and Tingli Ma**

In the past two decades considerable scientific and industrial attention has been focused on dye-sensitized solar cells (DSCs) because of the low cost, environmental friendliness, and simple preparation procedures for various photovoltaic devices. Typically, a DSC comprises a dye-sensitized nanocrystalline semiconductor electrode (TiO_2), an electrolyte with a redox couple (triiodide/iodide), and a counter electrode (CE), in which triiodide is reduced to iodide by the electrons flowing through the external circuit.[1]

A fluorine-doped tin oxide (FTO) glass loaded with Pt is a conventional CE with good electrocatalytic properties for the reduction of triiodide to iodide.[2] However, as a noble metal, Pt is scarce and expensive. Finding inexpensive substitutes for Pt as an alternative CE in the DSC system is therefore crucial. The normal approach is to replace Pt with abundant, nonprecious materials that are not susceptible to price inflation under high-demand circumstances.[3] Heretofore, several kinds of new materials, such as carbon materials and organic polymers, have been proposed to replace Pt.[4] Unfortunately, these materials have low catalytic activity, bad corrosion resistance to a corrosive redox couple in the electrolyte, and poor thermal stability. In recent studies, inorganic compounds such as CoS and TiN, which show electrocatalytic activity in reducing triiodide, have been applied in DSCs as the catalytic material in the CE.[5] Compared with carbon materials and organic polymers, the inorganic compounds display unique characteristics such as a broad variety of materials, a good plasticity, and a simple fabrication. Thus, the development and study of inorganic compounds as an alternative catalytic material to Pt in the DSC system may pave a promising way to reduce the cost of DSCs further and to make this system more competitive among various photovoltaic devices.

Transition-metal carbides are a potential substitute for Pt because of their low cost, high catalytic activity, selectivity, and good thermal stability under rigorous conditions. The redox mechanism and the high catalytic activity of metal carbides have been investigated in previous studies.[6] Tungsten carbide (WC) has been applied in polymer electrolyte membrane fuel cells since Levy and Boudart first addressed its Pt-like catalytic behavior, which is a consequence of its electronic structure.[7] Besides WC, some transition-metal carbides, such as molybdenum, vanadium, chromium, titanium, niobium, and tantalum carbides, have also been applied in the hydrogenation of aromatic hydrocarbon molecules and unsaturated alkenes.[8]

Herein, we attempt to replace Pt as the CE in the DSC system by several carbides. Composites of MoC and WC embedded in ordered nanomesoporous carbon materials (MoC-OMC, WC-OMC) were synthesized with a modified simple method (see the Supporting Information). Figure 1 a,b shows the surface morphologies of the blocky MoC-OMC and

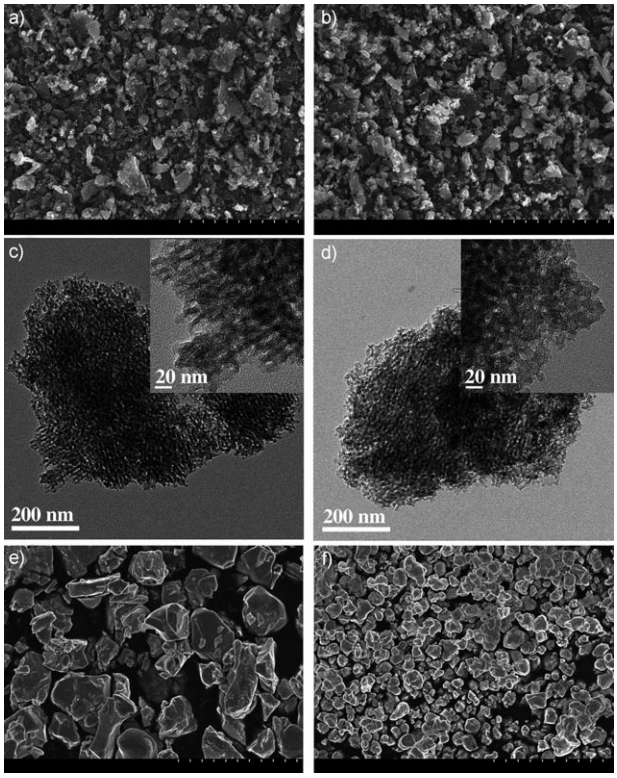

Figure 1. SEM images of a) MoC-OMC, b) WC-OMC, e) Mo_2C, and f) WC powders (scale bars = 5 μm); and TEM images of c) MoC-OMC and d) WC-OMC. The insets in (c) and (d) show magnified areas. The scale bars in (a), (b), (e), and (f) are 5 μm.

[*] Dr. M. X. Wu, M. Sc. X. Lin, Prof. T. L. Ma
State Key Laboratory of Fine Chemicals
Faculty of Chemicals, Environmental and Biological Science and Technology
Dalian University of Technology
No. 2 Linggong Road, Ganjingzi District, Dalian City
Liaoning Province 116024 (P. R. China)
Fax: (+86) 411-8498-6237
E-mail: tinglima@dlut.edu.cn
Homepage: http://finechem.dlut.edu.cn/matingli
Prof. A. Hagfeldt
Department of Physical and Analytical Chemistry
Uppsala University, Box 259, 75105 Uppsala (Sweden)

[**] This work was supported by the 863 Program (grant no. 2009AA03Z220) and the NSFC (grant no. 50773008).

Supporting information for this article is available on the WWW under http://dx.doi.org/10.1002/anie.201006635.

WC-OMC with an average size of 100 nm by scanning electron microscopy (SEM). In Figure 1c,d, the TEM images show that the blocky MoC-OMC and WC-OMC are built by ordered nanomesoporous carbon materials into which the MoC or WC particles are incorporated. The ordered nanomesoporous carbon materials consist of nano-sized carbon particles. The synthesized MoC-OMC and WC-OMC have large surface areas of 611 and 598 $m^2 g^{-1}$, respectively, as calculated by the Brunauer–Emmett–Teller (BET) method. The large surface area is crucial for high catalytic activity. The XRD patterns of the synthesized MoC-OMC and WC-OMC are shown in Figure S1a in the Supporting Information. In addition, we evaluated the effects of the amounts of the precursors (ammonium heptamolybdate or ammonium paratungstate) on 1) the crystallinity, 2) the sintering temperature, which influences the crystallinity, and 3) the catalytic activity, which is also affected by the crystallinity (see the Supporting Information, Figures S1 and S2). For comparison, we also used purchased Mo_2C and WC powders as CEs to fabricate DSCs. Figure 1e,f shows the surface morphologies of the purchased pure Mo_2C and WC powders, respectively. We calculated particle sizes for the Mo_2C and WC powders of 300 and 190 nm by using the data obtained from BET surface area experiments.

MoC-OMC, WC-OMC, Mo_2C, and WC electrodes were prepared on a FTO glass with a spray-coating technique developed by our group.[9] To characterize the catalytic activity of the MoC-OMC, WC-OMC, Mo_2C, and WC electrodes (Figure S3 in the Supporting Information) cyclic voltammetry (CV) experiments were carried out. For comparison, we also measured the cyclic voltammograms of the Pt and the carbon dye (CD) electrodes under the same conditions. (CD is a low-cost carbon material abstracted from coal tar.) Two pairs of redox peaks were observed for the Pt, CD, MoC-OMC, WC-OMC, and Mo_2C electrodes. The relative negative pair was assigned to redox reaction (1) [Eq. (1)] and the positive pair was assigned to redox reaction (2) [Eq. (2)].[10] In contrast, only one pair of redox peaks assigned to Equation (1) was observed for the WC electrode.

$$I_3^- + 2e^- \rightleftharpoons 3I^- \quad (1)$$

$$3I_2 + 2e^- \rightleftharpoons 2I_3^- \quad (2)$$

Compared with the four other electrodes, the MoC-OMC and WC-OMC electrodes exhibit large current densities, which implies huge surface areas and high electrocatalytic activities. The cathodic peaks of the Mo_2C and the WC electrodes which correspond to Equation (1) exhibit a more negative potential than those of the Pt and CD electrodes, and thus they show that Mo_2C and WC can effectively catalyze the reduction of triiodide to iodide.[4f] Based on the CV analysis, MoC-OMC, WC-OMC, Mo_2C, and WC are expected to perform as well as Pt in DSCs.

Figure 2a shows the photocurrent–voltage curves of three DSCs using MoC-OMC, WC-OMC, and Pt electrodes as CEs. As shown in Table 1, the devices equipped with MoC-OMC and WC-OMC CEs yield energy conversion efficiencies (η) of

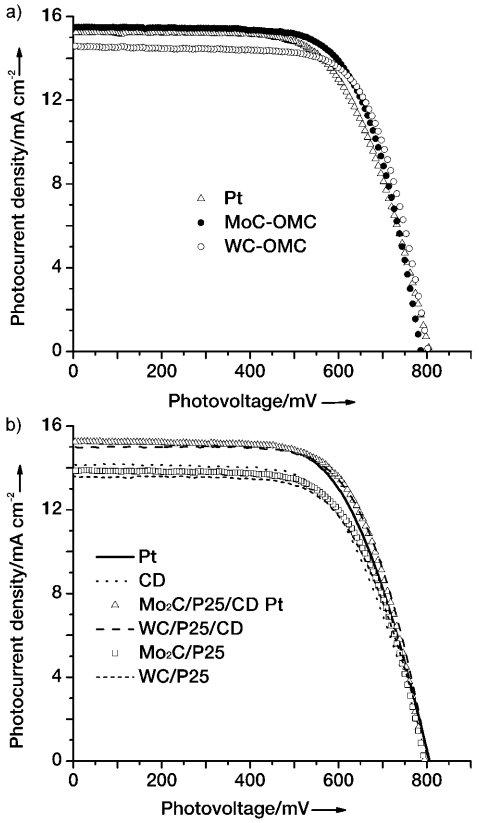

Figure 2. a) Photocurrent–voltage curves of DSCs with MoC-OMC, WC-OMC, and Pt CEs; b) Photocurrent–voltage curves of DSCs with Pt, CD, Mo_2C/P25/CD, Mo_2C/P25, WC/P25/CD, and WC/P25 CEs. Mo_2C/P25/CD, Mo_2C/P25, WC/P25/CD, and WC/P25 electrodes were prepared under optimized conditions (see the Supporting Information).

Table 1: Photovoltaic performance of DSCs with different CEs[a] and EIS parameters of the dummy cell assembled with two identical CEs.[b]

Sample	J_{sc} [mA cm^{-2}]	V_{oc} [mV]	*FF*	η [%]	R_s [Ω]	R_{ct} [Ω]	*CPE* [μF]
Pt	15.23	807	0.64	7.89	16.5	2.2	4.8
CD	14.18	805	0.63	7.20	20.9	2.4	25.3
MoC-OMC	15.50	787	0.68	8.34	17.1	1.3	38.2
WC-OMC	14.59	804	0.70	8.18	17.4	1.5	34.9
Mo_2C/P25/CD	15.25	796	0.67	8.14	17.7	1.7	27.3
WC/P25/CD	14.93	810	0.66	8.03	17.4	1.8	31.8
Mo_2C/P25	13.87	795	0.65	7.22	18.5	2.5	24.5
WC/P25	13.59	806	0.65	7.08	18.8	2.9	29.4

[a] J_{sc}: short-circuit current density; V_{oc}: open-circuit voltage; *FF*: fill factor; η: energy conversion efficiency. [b] R_s: series resistance; R_{ct}: charge-transfer resistance at the CE/electrolyte interface; *CPE*: constant phase angle element.

8.34 and 8.18%, respectively, which are superior to that of the device with a Pt CE (7.89%). Thus, the high catalytic activity of MoC-OMC and WC-OMC is validated.

To compare the catalytic activity of these CEs, we assembled two DSCs equipped with pure Mo_2C and WC CEs, named device A and B. The energy conversion efficiencies of the devices, 5.70 and 5.35% (Figure S4 in the Supporting Information), are lower than those of the devices

equipped with MoC-OMC and WC-OMC. The decreased efficiencies result from the large size of the purchased pure Mo_2C and WC particles, which tend to aggregate and subsequently show low catalytic surface area, bad conductivity, and weak bonding to the FTO glass substrate.

To avoid particle aggregation and to improve the bonding, various amounts (10, 20, 50, 100, and 200 mg) of TiO_2 powder (P25) were added to the Mo_2C and WC paste and the optimum amount of P25 was determined. As shown in Table S1 in the Supporting Information, the devices using Mo_2C/P25 and WC/P25 CEs with 50 mg P25 yield the highest efficiencies, 7.22 and 7.08%, respectively, which are 27 and 32% higher than the corresponding efficiencies of the devices using Mo_2C and WC CEs without P25 (Figure S5 and experimental details are provided in the Supporting Information). To improve the conductivity of the Mo_2C/P25 and WC/P25 electrodes, the optimum amount of CD was also determined by adding various amounts of CD (10, 20, 50, and 100 mg) to the Mo_2C/P25 and WC/P25 pastes. Figure S6 in the Supporting Information shows the photocurrent–voltage curves of the DSCs using Mo_2C/P25/CD and WC/P25/CD electrodes with various amounts of CD. The devices using Mo_2C/P25/CD and WC/P25/CD CEs with 50 mg P25 and 50 mg CD yield the highest efficiencies of 8.14 and 8.03%, respectively. These values are 43 and 50% greater than the efficiencies of the devices using pure Mo_2C and WC CEs (Table S2 in the Supporting Information).

After the preparation conditions of the Mo_2C and the WC CEs had been optimized, the Mo_2C/P25/CD and WC/P25/CD CEs match the performance of the Pt CE. Figure 2b summarizes the photocurrent–voltage curves of the DSCs with Mo_2C and WC CEs prepared under optimum conditions. The corresponding photovoltaic parameters are listed in Table 1. We confirmed that MoC-OMC and WC-OMC exhibit excellent catalytic activities and that they also show decent catalytic activity in reducing triiodide. The addition of P25 and CD to Mo_2C and WC greatly improves the catalytic properties.

To reveal the electrochemical characteristics of the MoC-OMC, WC-OMC, Mo_2C, and WC electrodes, electrochemical impendence spectroscopy (EIS) experiments were carried out with dummy cells fabricated with two identical electrodes (CE//IL//CE). In Figure 3, the high-frequency intercept on the real axis represents the series resistance (R_s). Two maxima in the middle- and low-frequency regions arise from the charge-transfer resistance (R_{ct}) and the corresponding constant phase angle element (*CPE*) at the CE/electrolyte interface, and the Nernst diffusion impedance of the triiodide/iodide couple in the electrolyte, respectively.[11] The R_{ct} value is calculated by fitting the left-hand hump, and it varies inversely with the electrocatalytic activity for the reduction of triiodide.[12] The small R_s values of the MoC-OMC and WC-OMC electrodes (Table 1) indicate that the Mo_2C and WC particles are firmly bonded to the substrate. Addition of TiO_2 particles (P25; <100 mg) reduces the R_s of the Mo_2C and the WC electrodes (Figure S7a,b in the Supporting Information). P25 plays the role of a binder and improves the bonding of the Mo_2C or the WC particles to the FTO glass substrate. This can facilitate electron transmission across the CE/substrate interface (see Table S3 in the Supporting Information). In Table 1, the R_{ct} of MoC-OMC and WC-OMC are 1.3 and 1.5 Ω smaller than the R_{ct} of Pt. The two electrodes have the largest *CPE* and possess good catalytic activity and large surface areas, as already observed in the CV experiments.[13] The addition of P25 reduces the R_{ct} of the Mo_2C and WC electrodes. Apart from improving the bonding of the Mo_2C or the WC particles to the substrate, the addition of P25 also directly prevents the Mo_2C and WC particles from aggregation which leads to large catalytic active areas. The addition of excessive P25, however, lowers the catalytic activity, which is characterized by a large R_s and R_{ct} of the Mo_2C/P25 and WC/P25 electrodes and arises from the poor conductivity of the CEs (see Figure S7a,c as well as Table S3 in the Supporting Information). The addition of CD reduces R_s and R_{ct} owing to the improved conductivity of the CEs. Figure S8a,c in the Supporting Information shows the Nyquist plots of the dummy cells with Mo_2C and WC at various amounts of CD (see Table S4 in the Supporting Information). The EIS results agree with the photocurrent–voltage experiments.

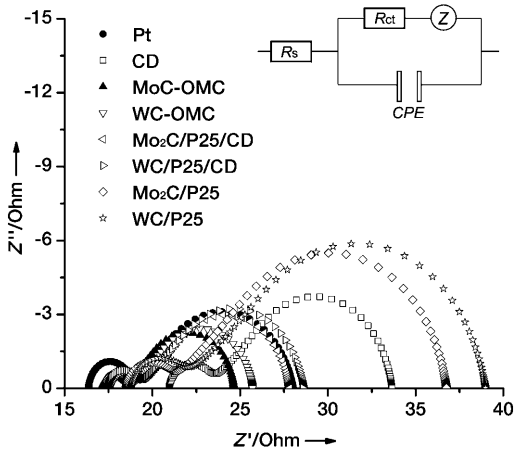

Figure 3. Nyquist plots of the dummy cell fabricated with two identical Pt(●), CD (□), MoC-OMC (▲), WC-OMC (▽), Mo_2C/P25/CD (◁), WC/P25/CD (▷), Mo_2C/P25 (◇), and WC/P25 (☆) electrodes. The frequency range was set from 100 mHz to 1 MHz, and the amplitude of the alternating current was set to 10 mV. The inset shows the corresponding circuit.

To further examine the interfacial charge-transfer properties of the triiodide/iodide couple on the electrode surface. Tafel polarization measurements were carried out in a dummy cell similar to the one used in the EIS experiments. Figure 4 shows the logarithmic current density ($\log J$) as a function of the voltage (U) for the oxidation/reduction of triiodide to iodide. The anodic and cathodic branches of the MoC-OMC, WC-OMC, Mo_2C/P25/Cd, and WC/P25/Cd electrodes show a larger slope than the conventional Pt and CD electrodes which indicates the presence of a large exchange current density (J_0) on the electrode surfaces. These results confirm that the catalytic activity of MoC-OMC, WC-OMC, Mo_2C, and WC is sufficient to catalyze the reduction of triiodide to iodide.[14]

We have found that the addition of P25 and CD to Mo_2C or WC electrodes improves not only the J_0, but also the limiting current density (J_{lim}). The optimum amounts of P25

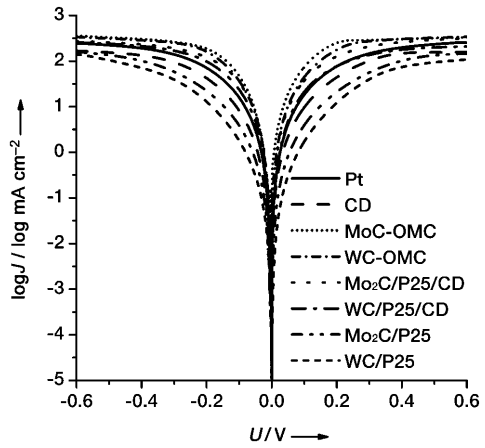

Figure 4. Tafel curves of different dummy cells that are similar to the ones used for the EIS measurements.

and CD added to the CEs were determined by Tafel polarization analysis (Figures S7b,d and S8b,d in the Supporting Information). The J_{lim} depends on the diffusion coefficient of the triiodide/iodide redox couple in the DSC system.[15] In Figure 4, the J_{lim} values of the eight electrodes are of the same magnitude. This finding indicates that there is a similar diffusion coefficient in the symmetrical dummy cell according to Equation (3), where D is the diffusion coefficient of the triiodide, l is the spacer thickness, n is the number of electrons involved in the reduction of triiodide at the electrode, F is the Faraday constant, and C is the triiodide concentration.

$$D = \frac{l}{2nFC} J_{lim} \tag{3}$$

In addition, J_0 can be obtained by Equation (4), where R_{ct} is extracted from the electrochemical impendence spectra, T is the temperature, R is the gas constant, and n is the total number of individuals. The tendency of J_0 to vary on different CE surfaces as described by Equation (4) is in accordance with the results of the Tafel curve plots.[5a,15]

$$J_0 = \frac{RT}{nFR_{ct}} \tag{4}$$

We have successfully developed several carbide-based catalysts—MoC-OMC, WC-OMC, Mo_2C, and WC—for the reduction of triiodide in the DSC system. CV, EIS, Tafel polarization, and photocurrent–voltage analysis confirm the excellent catalytic activities of the synthesized MoC-OMC and WC-OMC composites, which are comparable to that of the expensive Pt catalyst prepared by a pyrolysis method. The purchased Mo_2C and WC particles also catalyze effectively the reduction of triiodide to iodide despite their large particle size. Furthermore, the results show that the addition of P25 and CD improves the adhesion, the catalytic activity, and the conductivity of the Mo_2C and WC electrodes. The optimum amounts of P25 and CD added to the CEs were also determined. Our results demonstrate that molybdenum and tungsten carbide are potential alternatives to the expensive and scarce Pt CE for low-cost DSCs.

Experimental Section

The experimental details for the preparation of metal carbides and the fabrication of DSCs are described in the Supporting Information.

The X-ray diffraction experiments were carried out with an automatic X-ray powder diffractometer (D/Max 2400, RIGAKU). Nitrogen adsorption–desorption isotherms were measured with an Antosorb-1 Apparatus (Antosorb-1, Quantachrome, USA) to determine the BET surface areas of MoC-OMC and WC-OMC as well as pure Mo_2C and WC powder. The morphologies of the MoC-OMC and the WC-OMC as well as the pure Mo_2C and the WC surfaces were characterized by SEM (FEI HITACHI S-4800). The morphologies of MoC-OMC and WC-OMC were also characterized by TEM (Tecnai G^2 Spirit). Cyclic voltammetry (CV) was carried out in a three-electrode system in an Ar-purged acetonitrile solution of 0.1 M $LiClO_4$, 10 mM LiI, and 1 mM I_2 at a scan rate of 100 mV s^{-1} by using a BAS 100B/W electrochemical analyzer. Platinum served as a counter electrode and the Ag/Ag^+ couple was used as a reference electrode. The photocurrent–voltage performance of the DSCs was measured with a Keithley digital source meter (Keithley 2601, USA) and simulated under AM 1.5 illumination ($I = 100$ mW cm^{-2}, Solar Light Co., INC., USA). The EIS experiments were conducted in dummy cells by using a computer-controlled potentiostat (Zenium Zahner, Germany) in the dark. The measured frequency ranged from 100 mHz to 1 MHz, and the amplitude of the alternating current was set at 10 mV. The spectra were fitted by the Zview software. The equivalent circuit diagram is shown in Figure 3. Tafel polarization measurements were carried out with an electrochemical work station system (LK-9805, Tianjin Lanli Inc.) in a dummy cell with a scan rate of 50 mV s^{-1}.

Received: October 22, 2010
Revised: January 18, 2011
Published online: March 11, 2011

Keywords: carbides · dye/pigments · energy conversion · photochemistry · solar cells

[1] a) B. O' Regan, M. Grätzel, *Nature* **1991**, *353*, 737; b) M. Grätzel, *Nature* **2001**, *414*, 338; c) J. H. Wu, S. C. Hao, Z. Lan, J. M. Lin, M. L. Huang, Y. F. Huang, P. J. Li, T. Sato, *J. Am. Chem. Soc.* **2008**, *130*, 11568.

[2] a) H. Yu, S. Q. Zhang, H. J. Zhao, G. Will, P. Liu, *Electrochim. Acta* **2009**, *54*, 1319; b) K.-H. Park, M. Dhayal, *Electrochem. Commun.* **2009**, *11*, 75; c) X. M. Fang, T. L. Ma, G. Q. Guan, M. Akiyama, T. Kida, E. Abe, *J. Electroanal. Chem.* **2004**, *570*, 257; d) X. M. Fang, T. L. Ma, G. Q. Guan, M. Akiyama, E. Abe, *J. Photochem. Photobiol. A* **2004**, *164*, 179.

[3] R. Bashyam, P. Zelenay, *Nature* **2006**, *443*, 63.

[4] a) E. Ramasamy, W. J. Lee, D. Y. Lee, J. S. Song, *Appl. Phys. Lett.* **2007**, *90*, 173103; b) E. Ramasamy, W. J. Lee, D. Y. Lee, J. S. Song, *Electrochem. Commun.* **2008**, *10*, 1087; c) P. Joshi, Y. Xie, M. Ropp, D. Galipeau, S. Bailey, Q. Q. Qiao, *Energy Environ. Sci.* **2009**, *2*, 426; d) Q. H. Li, J. H. Wu, Q. W. Tang, Z. Lan, P. J. Li, J. M. Lin, L. Q. Fan, *Electrochem. Commun.* **2008**, *10*, 1299; e) W. J. Hong, Y. X. Xu, G. W. Lu, C. Li, G. Q. Shi, *Electrochem. Commun.* **2008**, *10*, 1555; f) J. H. Wu, Q. H. Li, L. Q. Fan, Z. Lan, P. J. Li, J. M. Lin, S. C. Hao, *J. Power Sources* **2008**, *181*, 172.

[5] a) M. K. Wang, A. M. Anghel, B. Marsan, N. C. Ha, N. Pootrakulchote, S. M. Zakeeruddin, M. Grätzel, *J. Am. Chem. Soc.* **2009**, *131*, 15976; b) Q. W. Jiang, G. R. Li, X. P. Gao, *Chem. Commun.* **2009**, 6720; c) G. R. Li, F. Wang, Q. W. Jiang, X. P.

Gao, P. W. Shen, *Angew. Chem.* **2010**, *122*, 3735; *Angew. Chem. Int. Ed.* **2010**, *49*, 3653.
[6] a) J. G. Chen, C. M. Kirn, B. Frühberger, B. D. Devries, M. S. Touvelle, *Surf. Sci.* **1994**, *321*, 145; b) R. J. Colton, J. J. Huang, J. W. Rabalais, *Chem. Phys. Lett.* **1975**, *34*, 337; c) S. T. Oyama, *Catal. Today* **1992**, *15*, 179.
[7] a) R. B. Levy, M. Boudart, *Science* **1973**, *181*, 547; b) Y. Hara, N. Minami, H. Matsumoto, H. Itagaki, *Appl. Catal. A* **2007**, *332*, 289.
[8] a) J. D. Oxley, M. M. Mdleleni, K. S. Suslick, *Catal. Today* **2004**, *88*, 139; b) Y. Li, Y. Fan, Y. Chen, *Catal. Lett.* **2002**, *82*, 111; c) P. Da Costa, J.-L. Lemberton, C. Potvin, J.-M. Manoli, G. Perot, M. Breysse, G. Djega-Mariadassou, *Catal. Today* **2001**, *65*, 195; d) R. Ganesan, J. S. Lee, *Angew. Chem.* **2005**, *117*, 6715; *Angew. Chem. Int. Ed.* **2005**, *44*, 6557; e) N. I. Il′chenko, *Kinet. Katal.* **1977**, *18*, 153.
[9] L. Yang, L. Q. Wu, M. X. Wu, G. Xin, H. Lin, T. L. Ma, *Electrochem. Commun.* **2010**, *12*, 1000.
[10] A. I. Popov, D. H. Geske, *J. Am. Chem. Soc.* **1958**, *80*, 1340.
[11] a) Q. Wang, J.-E. Moser, M. Grätzel, *J. Phys. Chem. B* **2005**, *109*, 14945; b) J. van de Lagemaat, N.-G. Park, A. J. Frank, *J. Phys. Chem. B* **2000**, *104*, 2044; c) R. Kern, R. Sastrawan, J. Ferber, R. Stangl, J. Luther, *Electrochim. Acta* **2002**, *47*, 4213.
[12] J. K. Chen, K. X. Li, Y. H. Luo, X. Z. Guo, D. M. Li, M. H. Deng, S. Q. Huang, Q. B. Meng, *Carbon* **2009**, *47*, 2704.
[13] J. Bisquert, M. Grätzel, Q. Wang, F. Fabregat-Santiago, *J. Phys. Chem. B* **2006**, *110*, 11284.
[14] A. Hauch, A. Georg, *Electrochim. Acta* **2001**, *46*, 3457.
[15] S. M. Zakeeruddin, M. Grätzel, *Adv. Funct. Mater.* **2009**, *19*, 2187.

